Available online at www.sciencedirect.com
SCIENCE DIRECT®
Physica B 350 (2004) 231–238
PHYSICA B
www.elsevier.com/locate/physb

Short-time single particle dynamics in quantum and molecular systems

Carla Andreani[a,b,*]

[a] Dipartimento di Fisica, Universitá degli Studi di Roma Tor Vergata, Via R. Scientifica 1, 00133 Rome, Italy
[b] Istituto Nazionale per la Fisica della Materia, Corso Perrone 24, 16152 Genova, Italy

Abstract

Recent experimental and theoretical results on the short-time single particle dynamics of atomic and molecular systems are reviewed. Results on momentum distribution, $n(p)$, and single particle mean kinetic energy, $\langle E_k \rangle$, are presented, both in atomic (quantum) systems such as ^{3}He and ^{4}He in the normal and superfluid state, and in molecular systems such as H_2, H_2S and H_2O. The main experimental technique employed for these measurements is known as deep inelastic neutron scattering, i.e. neutron scattering at high wavevector and energy transfers. This is the only experimental technique which allows the direct measurement of $n(p)$ and $\langle E_k \rangle$, interesting physical quantities in any systems where the short-time dynamic behavior departs from the classical one.

PACS: 61.12.Ex; 61.25.Em

Keywords: Quantum systems; Molecular systems; Deep inelastic neutron scattering

1. Introduction

The short-time dynamics of single atoms and molecules in the liquid and solid phases has always attracted the interest of both theoretical and experimental physicists. The reason is the fundamental scientific interest of these studies, especially in quantum systems. Indeed, the single particle dynamics and related quantities, such as the single particle mean kinetic energy, $\langle E_k \rangle$, and momentum distribution, $n(p)$, are of great importance in a variety of systems: quantum systems such as ^{3}He, ^{4}He and ^{3}He/^{4}He mixtures, molecular systems (in solid and liquid phases), strongly interacting electron systems, and system of nucleons in atomic nuclei [1]. In particular, the study of the dense phases of the two helium isotopes, in the normal and superfluid phases, has always attracted great attention by both theoreticians and experimentalists, these systems being considered as the prototypes of many-body systems of both bosons (^{4}He) and fermions (^{3}He). In the case of classical systems, the single particle momentum distribution is well described by the Maxwell–Boltzmann

*Corresponding author. Dipartimento di Fisica, Universitá degli Studi di Roma Tor Vergata, Via R. Scientifica 1, Rome 00133, Italy. Tel.: +39-06-72594441; fax: +39-06-2023507.
E-mail address: carla.andreani@roma2.infn.it (C. Andreani).

0921-4526/$ - see front matter © 2004 Elsevier B.V. All rights reserved.
doi:10.1016/j.physb.2004.04.035

function, whereas in other cases one obtains different $n(p)$ depending upon the specific nature of the system under study and the relative magnitude of the quantum mechanical effects [2].

Currently, the most direct and effective experimental technique which probes single particle dynamics in condensed matter systems is known as deep inelastic neutron scattering (DINS), or neutron Compton scattering, in analogy with the traditional Compton scattering of photons from electrons. DINS is at present the unique and effective technique for deriving *single particle momentum distributions*, $n(\boldsymbol{p})$ in condensed matter. It is based on the impulse approximation (IA) [3] which is exact in the limit of infinite momentum transfer. The IA states that if the momentum lost by the incident neutron is sufficiently large, scattering occurs from a single atom, which recoils in free dynamical conditions, with conservation of kinetic energy and momentum. For this approximation to be valid, the energy transfer to the recoiling atom must greatly exceed its interatomic binding energy. In a molecular system the applicability of the IA can be divided into two distinct regimes corresponding to sufficiently well separated energy scales for the intra-molecular and inter-molecular motions [4].

Two different deviations from IA, occur in an atomic system: those arising, at finite q values, from the interaction of the scattered particle with the neighbouring atoms surrounding the struck one are known as final state effects (FSE) [5]; those arising from the bound nature of the initial state, are known as initial state effect (ISE) [6].

The scattering regime of high momentum and energy transfers requires the use of epithermal neutrons, i.e. neutrons where the incident energies is in excess of 1 eV, in order to keep deviations from the IA small. These are readily obtainable from pulsed neutron sources such as the ISIS facility. Conventional inelastic spectrometers, working in direct geometry, are usually restricted to operate at energy transfer below 1 eV by the low reflectivity of the crystal analysers and by the low transmission of the choppers. The suitable experimental configuration for an effective DINS study is an inelastic neutron spectrometer operating in inverse geometry on a pulsed source. Examples with this technique on the VESUVIO spectrometer at the ISIS facility are compared with the same quantities derived from Path Integral Monte Carlo simulations.

2. Momentum distributions

It is worthwhile noting that *single particle momentum distributions*, $n(\boldsymbol{p})$, and *mean kinetic energies*, $\langle E_k \rangle$, are both physical quantities which strongly characterise any condensed matter system where the short-time dynamical behaviour departs from the classical one. We recall that

$$\langle E_k \rangle = \frac{1}{2M} \int n(\boldsymbol{p}) p^2 \, \mathrm{d}\boldsymbol{p},$$

M being the mass of the particle considered. The physical meaning of the momentum distribution is clear by considering its relation with the single particle wave function, $\Psi(\boldsymbol{r})$, i.e.

$$n(\boldsymbol{p}) = \frac{1}{(2\pi)^3} \left| \int \Psi(\boldsymbol{r}) \exp[\mathrm{i}\boldsymbol{p}\,\boldsymbol{r}] \, \mathrm{d}\boldsymbol{r} \right|^2.$$

Measurements of $n(\boldsymbol{p})$ can be used to determine the wave function, in analogy to the determination of a real-space structure from diffraction pattern. Both quantities, $n(\boldsymbol{p})$ and $\langle E_k \rangle$ are substantially different according to the system investigated and/or the approximations adopted (e.g. the classical Maxwellian regime, the quantum Boltzmann liquid regime, the Debye-like harmonic crystal, the Bose condensate, Fermi liquids etc.). In quantum systems the de Broglie wavelength of a particle, λ_{dB}, associated with the single particle motion can be larger than the inter-particle spacing [8]. Another interesting object is the de Boer's quantum parameter $\Lambda = (2\hbar/\sigma)(M\varepsilon)^{1/2}$. It measures the competition between the delocalising effect of the kinetic energy operator on the energy eigenfunctions and the localising effect of the attractive part of the potential (σ and ε being the atomic diameter and the two-particle relative energy of the hard core or a Lennard Jones (LJ) potential, respectively). Thus in quantum systems the zero point motion is more important for larger Λ values and represents a relevant fraction of the total energy at low temperature. Weak quantum

systems are those where λ_{dB} is lower than average inter-particle distance, d, or where it is lower than inter-particle potential radius, given by the σ of the LJ potential. In the former case, one can neglect exchange effects among particles whereas in the latter case quantum delocalisation can be disregarded. In reality, almost all quantum fluids at low temperature can be regarded as weak quantum systems, with few exceptions such as ^{3}He, ^{4}He and ^{3}He/^{4}He mixtures.

In classical systems the spectral weight of the density response occurs in the frequency region $k_B T \gg \hbar\omega$ (T being the temperature of the system) with the occupancy of any momentum state always much less than unity. The opposite inequality holds in quantum systems, i.e. $\hbar\omega \gg k_B T$, and upon lowering the temperature, the occupancy of some one-body momentum states starts to approach unity and details of the different quantum statistics become visible. A direct consequence of the zero point motion in quantum systems clearly emerges in the momentum distribution function $n(p)$: although there is no general result for this function it appears that it changes in such a way that $\langle E_k \rangle$ is always greater than the classical value $3/2k_B T$. In weakly quantum systems corrections of the order of $\hbar^2$ can be incorporated into the $n(p)$ function so that a Gaussian lineshape is still retained, but the temperature parameter T is replaced by an effective temperature $T_{eff} > T$. In systems composed of pure helium isotopes and their mixture, the different $n(\boldsymbol{p})$ distribution functions start to deviate from the Maxwell–Boltzmann line shape, depending on the specific nature and relative magnitude of the quantum mechanical effects [8]. In a gas composed of particles with half-integer spin the antisymmetry requirement for fermions leads to the Fermi–Dirac distribution, which at zero temperature for non-interacting particles, gives $n(\boldsymbol{p}) = 1$ for $p < p_f$ and $n(\boldsymbol{p}) = 0$ for $p > p_f$, p_f being the momentum at the Fermi surface. The corresponding scattering law $S(q, \omega)$ is a parabola. For the interacting case, such as liquid ^{3}He, $n(\boldsymbol{p})$ is expected to show a discontinuity at p_f giving rise to a discontinuity in the slope of $S(q,\omega)$ at $\omega = q^2/2M \pm qp_f/M$. For the ideal Fermi gas the parabola also approaches zero at these values. For a gas of bosons a certain fraction condenses into a state of zero momentum below a temperature T_λ (namely the λ transition). It is generally accepted that the occurrence of superfluidity in ^{4}He is associated with the presence of a Bose condensate, in which a macroscopic number of particles occupies a single momentum state at $p = 0$.

The momentum distribution is traditionally separated into two components: $n(p) = (2\pi)^3 r n_0 \delta(p) + n'(p)$, where n_0 the condensate fraction, and $n'(p)$, the non-condensate fraction are given by

$$n_o = \lim_{r \to \infty} \frac{\rho_1(r)}{\rho};$$

$$n'(p) = \int \left[\rho_1(r) - \rho_1(\infty)\right] e^{ipr}\, dr,$$

where $\rho(r)$ represents the one-body density matrix, which is related to the momentum distribution of the normal component, $n'(p)$, via a Fourier transform. The condensate gives rise to a δ-function spike on both $n(p)$ and $S(q,\omega)$ below the λ transition temperature [1].

Let us now look at the momentum distribution in a molecular system, starting from diatomic molecules where $n_i(\boldsymbol{k}_i)$ is the momentum distribution of the single atom within the molecule. In such a system it can be shown that it is possible to decouple the total wave function into two distinct wave functions, one describing the centre of mass motion, $\Phi(R)$, and the other describing the relative motion of the two nuclei in the molecule, $\phi(r)$. This allows us to express $n_i(\boldsymbol{k}_i)$ as a convolution of two distinct functions, i.e. $N(\boldsymbol{k})$ and $n(\boldsymbol{k})$, describing the momentum distribution of the centre of mass and the relative motion, respectively. In a classical system $N(\boldsymbol{k})$ has a Gaussian form. It is important to stress that in a "weak" quantum system $N(\boldsymbol{k})$ also retains a Gaussian form, although the relationship between $\langle E_k \rangle$ and T, is more complex and usually expressed, as for atomic systems in terms of T_{eff} [1,8]. This occurs for example in simple fluids such as Ne [9] in ^{4}He [10,11], far away from the λ transition (for $T > 10$ K), and in fluids H_2 and D_2 [12,13], as described in the following sections. The theoretical momentum distribution, $n(\boldsymbol{k})$, for the relative motion of deuterium nuclei and the total

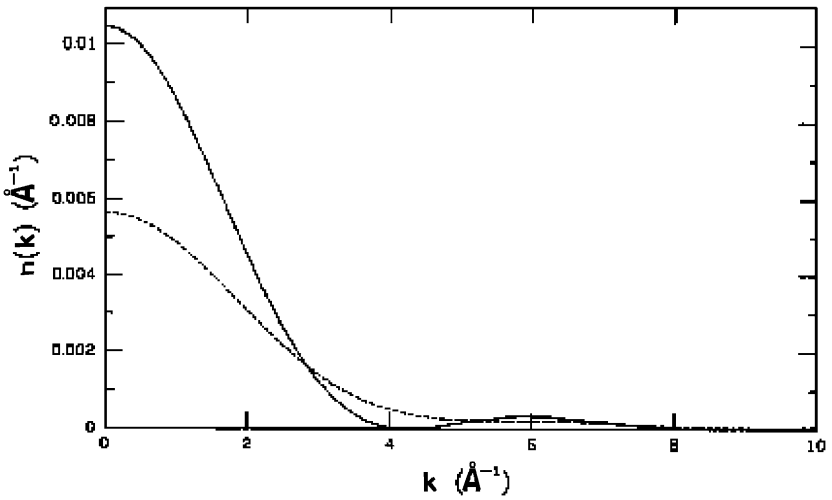

Fig. 1. Liquid D_2: $n(\boldsymbol{k})$ (solid line) and $n_i(\boldsymbol{k}_i)$ (dashed line), momentum distribution functions for the relative and total motion, respectively [12].

momentum distribution, $n_i(\boldsymbol{k}_i)$, of the deuterium nucleus, in D_2 are plotted in Fig. 1 [12].

3. Theoretical framework

Consider an event in which a neutron loses momentum $\boldsymbol{q}$ and energy ω scattering from an atom with mass M. If $\boldsymbol{p}$ is the momentum of the atom before the collision, after the collision the conservation of momentum yields $\boldsymbol{p}+\boldsymbol{q}$ and the conservation of energy $\omega(\boldsymbol{p}+\boldsymbol{q})^2/2M-p^2/2M$. One can then introduce the component of the atomic momentum along the direction of $\boldsymbol{q}$, generally indicated by y, namely

$$y = \boldsymbol{p}\widehat{\boldsymbol{q}} = \frac{M}{q}\left(\omega - \frac{q^2}{2M}\right),$$

where $\widehat{\boldsymbol{q}}$ is the unit vector along the direction of $\boldsymbol{q}$. This link between ω and $\boldsymbol{q}$ is known as y-scaling [3]. In a DINS experiment one measures a large number of neutron-atom collisions building up a distribution function $F(\widehat{\boldsymbol{q}}, y)$ by recording, for each event, the direction of $\widehat{\boldsymbol{q}}$ and the value of y. For isotropic samples such as liquid, glasses, powders and amorphous materials, $F(\widehat{\boldsymbol{q}}, y)$ reduces to $F(y)$, giving the probability that an atom has momentum component y along an arbitrary direction in space. $F(y)$ (or $J(y)$) is also known as the *Neutron Compton Profile* (NCP). The mean kinetic energy is then related to $F(y)$ via:

$$\langle E_{\mathrm{k}} \rangle = \left(\frac{3}{2M}\right)\int_{-\infty}^{\infty} F(y)y^2 \,\mathrm{d}y.$$

In a scattering process where q is finite the response function retains a q dependence due to the existence of final state effects (FSE), i.e. to the confinement of the struck nucleus by the surrounding atoms through the inter-particle potential V. Owing to the uncertainty principle the momentum in the final state and hence the initial state is uncertain. The overall effect is that a broadening is introduced in the observed $F(y, q)$.

In the case of systems composed of freely-rotating molecules, two distinct regimes can be envisaged for the applicability of the IA [12,14]: (a) where the energy of the incident neutron is large compared to the average collective excitation energy, but lower than the energy of the minimum internal excitation of the single molecule; (b) where the energy transfer greatly exceeds the energy scale of internal excitations of the molecules. In (a) the freely-rotating molecular system recoils with a mass equal to mass of the molecule as a whole (M_{m}) and the response function consists of the sum of several replicas of a single molecular

Compton profile, $F_{tr}(y)$, yielding

$$F(y,q) = \sum_n f^2 n(q) F_{tr}\left(y - \frac{M_m E_n}{q}\right),$$

where $F_{tr}(y)$ is very similar to the $F(y)$ for a monatomic system, but shifted by the quantity $(M_m E_n/q)$ with E_n being the nth roto-vibrational excitation energy, weighted by the squared molecular form factor for the nth roto-vibrational excitation, $f_n^2(q)$. The mean kinetic energy of the translational motion of the molecule, $\langle E_k \rangle_T$, can be directly obtained from the second moment of $F_{tr}(y)$. In regime (b), scattering occurs from the recoiling masses of the constituent nuclei of the molecule (M_1) and two separate contributions must be considered in order to derive the total mean kinetic energy of an individual nucleus, $\langle E_k \rangle_1$, i.e.

$$\langle E_k \rangle_1 = \tfrac{1}{2}\left[\langle E_k \rangle_T + \langle E_k \rangle_{RV}\right],$$

where $\langle E_k \rangle_{RV}$ is the mean kinetic energy due to the roto-vibrational motion, and $\langle E_k \rangle_T$ the mean kinetic energy due to the translational motion of the molecule as a whole. In this case the NCP, $F(y)$, can be expressed in terms of a convolution of $F_{tr}(y)$ and $F_{in}(y)$, i.e.

$$F(y) = 2\int_{-\infty}^{\infty} F_{in}(y - y') F_{tr}(2y)\, dy',$$

where the internal NCP $F_{in}(y)$ is related to the relative motion of the nuclei in the molecule. Simultaneous knowledge of $F(y)$ and $F_{tr}(y)$ is of great relevance, since it allows to derive precise information about the contributions to $F(y)$ arising from internal motion, which are ultimately related to the wave function describing the relative motion of the nuclei within a molecule. It is also worth noting that deviations from the IA, in a molecular system in the scattering regime (b) are caused by the interactions of the recoiling nucleus during both its intra- (V_{in}) and inter-molecular (V_{tr}) motions. These deviations, known as Final State Effects (FSE) can be revealed by measuring the double differential neutron scattering cross-section in a wide range of q. The existence of two distinct regimes in freely rotating molecular systems has suggested a joint use of inelastic neutron scattering measurements at intermediate (INS) and high momentum transfers (DINS) as complementary techniques for the study of the single particle, atomic (regime (b)) and the molecular (regime (a)) dynamical processes.

4. Experimental technique

The basic element for the DINS measurements at eV energies on an inverse geometry instrument is the nuclear resonance absorption foil, used to select the final energy of the scattered neutrons. Currently on the VESUVIO spectrometer, operating at the ISIS facility, the experimental technique consists of cycling the foil in and out of the scattered neutron beam so that two measurements are taken, one with the foil between the sample and detector and one with the foil removed. The difference between these two data sets (i.e. the number of neutrons absorbed by the foil) is the experimental time of flight signal, which provides a measurement of the intensity of neutrons scattered from the sample with final energy E_1. Once E_1 is fixed, the time of flight technique allows to reconstruct the whole kinematics of the scattering process, i.e. $\boldsymbol{q}$ and ω, thus to determine $F(y)$ [7,15].

5. Momentum distributions $n(p)$ in helium isotopes: ^{4}He, ^{3}He and ^{3}He/^{4}He mixture

The rich phenomenology of the helium isotopes has in recent years motivated the detailed study of the $\langle E_k \rangle$ and $n(p)$ in ^{4}He (in normal liquid [2,10] and superfluid [11]), ^{3}He (dense fluid phases [16,17] and solid [17]) and ^{3}He/^{4}He mixtures [18] with both experimental, numerical and theoretical techniques. Highlights in ^{4}He include DINS measurements of the mean kinetic energy through the superfluid transition, in the wavevector transfers range $90\,\text{Å}^{-1} < q < 150\,\text{Å}^{-1}$. The $\langle E_k \rangle$ undergoes a marked decrease from a value of 16.2 K at a temperature of 2.5 K, to a value of 13.9 K at 1.3 K [11] and a recent line shape analysis of those spectra has confirmed the earlier observation [2] of a non-Gaussian component in $n(p)$. This result is compatible with the best theoretical predictions [19] (see Fig. 2).

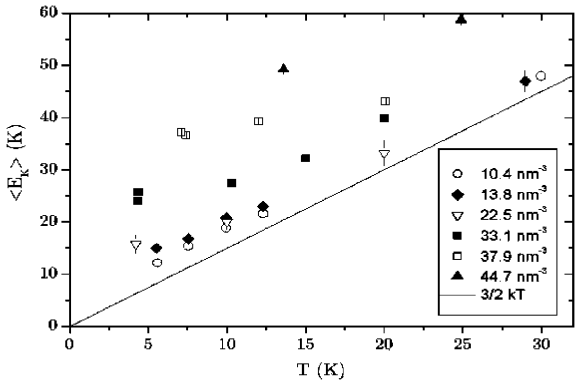

Fig. 2. Plots of $\langle E_k \rangle$ for fluid ^{4}He along different isochores as a function of T.

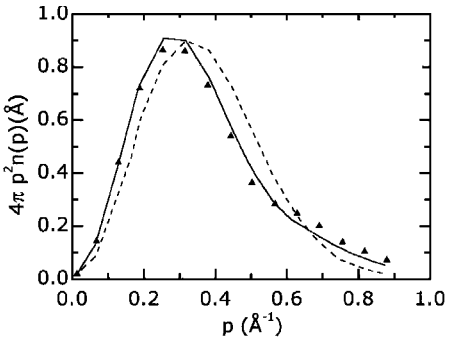

Fig. 3. Fluid ^{4}He at 2.5 K: $n(\boldsymbol{p})$ from Ref. [19] (triangles), $n(\boldsymbol{p})$ fitted from experimental data: purely Gaussian (dashed line) and also including non-Gaussian component (solid line).

A variety of experimental values for $\langle E_k \rangle$ are also now available on fluid ^{4}He in the normal phase, along supercritical isochors as a function of temperature (ref.), most of which are highlighted in Fig. 3.

The departure from the classical value of $\langle E_k \rangle$ is still visible at the lowest density and the zero point motion contribution is consistently seen to increase as a function of fluid density.

Recent studies on ^{3}He include the first determination of $\langle E_k \rangle$ in both BCC and HCP solid phases. The data were in excellent agreement with current molecular dynamic simulations, strongly supporting a microscopic dynamical description of the system, which includes both three-body interactions and anharmonic contributions [17]. For ^{3}He–^{4}He mixtures the interest arises from the presence of quantum exchange effects among particles obeying different statistics. The statistical disorder switches on a variety of new behaviours, such as a lowering of the superfluid transition temperature and the suppression of the superfluid fraction. DINS experimental measurements suggest: (a) a considerable increase of the Bose condensate fraction n_o, on the addition of ^{3}He; and (b) $\langle E_k \rangle$ values of the ^{3}He atoms in the mixture, which are consistent with a local environment of the atoms in the mixture quite different from current theoretical predictions [18].

6. Molecular systems (H_2, D_2, H_2S, H_2O)

Single particle (atomic and molecular) $n(\boldsymbol{p})$ and $\langle E_k \rangle$ in diatomic and heteronuclear molecular systems have been thoroughly studied both theoretically and experimentally. Diatomic homonuclear systems include para-H_2 and ortho-D_2 in dense phases, where both $\langle E_k \rangle_T$ [14] and $\langle E_k \rangle_{RV}$ [12,13] have been successfully measured and modelled by Monte Carlo simulation. For both these freely rotating molecular systems calculated response functions, using an approximate WKB [12] and exact quantum–mechanical models, have been successfully compared with the experimental data [20]. Calculations were performed both at finite values of momentum transfers, yielding $F(y, q)$, and at its asymptotic limit, $F(y)$. For the general case of freely rotating symmetric molecules an analytical expression for the momentum distribution has been given. It has been shown that, if the temperature of the system is large in comparison with the typical rotational energy, molecular rotations can be dealt with classically, while the vibrations must be described in a quantum way [12,13,21].

Reliable experimental values for $\langle E_k \rangle$ are available for H_2S, a system composed of freely rotating molecules [22], and H_2O [23]. In the former case DINS and inelastic neutron scattering (INS) studies have been performed in a wide thermodynamic interval, ranging from the solid phase to the liquid state. The results provide important quantitative indications for the relevance of molecular anisotropy

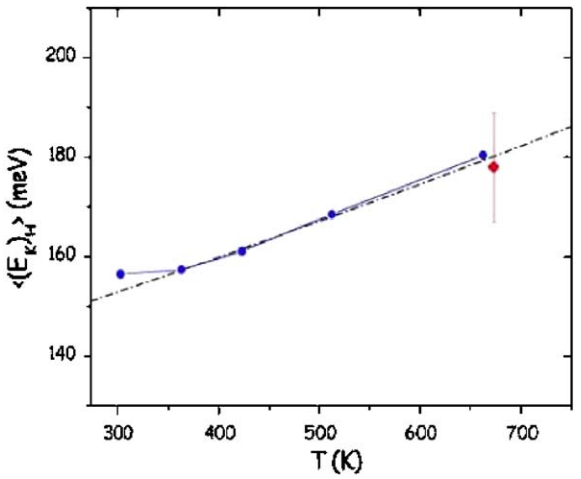

Fig. 4. H_2O, $\langle E_k \rangle$ vs. T: experiment at $T = 673.1$ K $p = 360$ bar (full square); optical data for isolated molecule (dot-dashed), dense fluid along coexistence curve and supercritical state (full circles) [23].

in determining the $\langle E_k \rangle_H$. For the first time, to our knowledge, a correct extraction of this quantity in a polyatomic molecular system, with an anisotropic momentum distribution function, has been achieved [22]. In the case of H_2O, DINS and INS experiments provided: (1) results in good agreement with the predictions of a harmonic model, under the assumptions of decoupling between translational, rotational and vibrational degrees of freedom (see Fig. 4) [23]; (2) and confirmed that an anisotropic momentum distribution is required for a satisfactory agreement with the experimental data.

7. Conclusions

The understanding of short-time dynamics in quantum systems is a challenging problem of fundamental interest. In this context DINS has provided unique information on the quantum nature of fermions and/or bosons and molecular systems. In this paper the most recent experimental results have been reviewed. In some cases a better microscopic understanding of the short-time dynamics has been achieved. The detailed knowledge of $\langle E_k \rangle$ and the determination of the $n(\boldsymbol{p})$ line shapes, hopefully in the near future, will shed more light on the microscopic features behind specta-

cular quantum effects, such as, for example: ^{4}He and ^{3}He superfluidity.

Acknowledgements

The author gratefully thanks Dr. D. Colognesi and Dr. R. Senesi, for stimulating discussions.

References

[1] P.C. Hohenberg, P.M. Platzmann. Phys. Rev. 152 (1966) 198; P.E. Sokol, R.N. Silver, J.W. Clark, in: R.N. Silver, P.E. Sokol (Eds.), Momentum Distributions, Plenum Press, New York, 1989, p. 1.
[2] K.H. Andersen, W.G. Stirling, H.R. Glyde, R.T. Azuah, S.M. Bennington, A.D. Taylor, Z.A. Bowden, I. Bailey, Physica B 197 (1994) 198;
K.H. Andersen, W.G. Stirling, H.R. Glyde, Phys. Rev. B 56 (1997) 8978.
[3] J.M.F. Gunn, C. Andreani, J. Mayers, J. Phys. C 19 (1986) L835;
E. Pace, G. Salme', G.B. West, Phys. Lett. B 273 (1991) 205.
[4] C. Andreani, D. Colognesi, A. Filabozzi, M. Nardone, E. Pace, Physica B 234 (1997) 329.
[5] H.R. Glyde, Phys. Rev. B 50 (1994) 6726.
[6] J. Mayers, C. Andreani, G. Baciocco, Phys. Rev. B 39 (1989) 2022.
[7] R. Senesi, et al., Physica B 276 (2000) 200.
[8] W.C. Kerr, K.S. Singwi, Phys. Rev. A 7 (1973) 1043.
[9] R.A. Cowley, A.D.B. Woods, Can. J. Phys. 49 (1971) 177.
[10] T.R. Sosnick, W.M. Snow, P.E. Sokol, Phys. Rev. B 41 (1990) 11185;
P. Martel, E.C. Svensson, A.D.B. Woods, V.F. Sears, R.A. Cowley, J. Low Temp. Phys. 23 (1976) 285;
C. Andreani, A. Filabozzi, M. Nardone, F.P. Ricci, J.C. Mayers, Phys. Rev. B 50 (1994) 12744;
U. Bafile, et al., Phys. Rev. Lett. 75 (1995) 1957;
D.M. Ceperley, R.O. Simmons, R.C. Blasdell, Phys. Rev. Lett. 77 (1996) 115.
[11] J. Mayers, C. Andreani, D. Colognesi, J. Phys.: Condens. Matter 9 (1997) 10639.
[12] Andreani, A. Filabozzi, E. Pace, Phys. Rev. B 51 (1995) 8854;
C. Andreani, D. Colognesi, E. Pace, Phys. Rev. B 60 (1999) 10008.
[13] C. Andreani, D. Colognesi, A. Filabozzi, E. Pace, M. Zoppi, J. Phys.: Condens. Matter 10 (1998) 7091.
[14] K.W. Herwig, J. Gavilano, M.C. Schmidt, O. Simmons, Phys. Rev. B 41 (1990) 96;
W. Langel, D.L. Price, R.O. Simmons, P.E. Sokol, Phys. Rev. B 38 (1988) 11275;
C. Andreani, et al., Europhys. Lett. 37 (1997) 329.

[15] C. Evans, J. Mayers, D.N. Timms, Phys. Rev. B 53 (1996) 3023.
[16] P.E. Sokol, K. Skold, D.L. Price, R. Kleb, Phys. Rev. Lett. 54 (1985) 909;
R.T. Azuah, et al., J. Low Temp. Phys. 101 (1995) 951.
[17] R. Senesi, C. Andreani, D. Colognesi, A. Cunsolo, M. Nardone, Phys. Rev. Lett. 86 (2001) 4584.
[18] R.T. Azuah, W.G. Stirling, J. Mayers, I.F. Bailey, P.E. Sokol, Phys. Rev. B 51 (1995) 6780;
Y. Wang, P.E. Sokol, Phys. Rev. Lett. 72 (1994) 1040;
R. Senesi, C. Andreani, A.L. Fielding, J. Mayers, W.G. Stirling, Phys. Rev. B 68 (2003) 214522.
[19] D.M. Ceperley, E.L. Pollock, Phys. Rev. Lett. 56 (1986) 351.
[20] C. Andreani, P. Cipriani, D. Colognesi, E. Pace, J. Phys.: Condens. Matter 12A (2000) 139.
[21] D. Colognesi, E. Pace, Physica B 293 (2001) 317.
[22] C. Andreani, E. Degiorgi, R. Senesi, F. Cilloco, D. Colognesi, J. Mayers, M. Nardone, E. Pace, J. Chem. Phys. 114 (2001) 387.
[23] C. Andreani, D. Colognesi, E. Degiorgi, M.A. Ricci, J. Chem. Phys. 115 (2001) 11243.